# Restricted Rotation Involving the Tetrahedral Carbon. LVII. Stereodynamics of 9-(2-Alkylphenoxy)-1,4-dimethyltriptycenes[1)]

Gaku Yamamoto* and Michinori Ōki
*Department of Chemistry, Faculty of Science, The University of Tokyo, Bunkyo-ku, Tokyo 113*

(Received February 26, 1985)

1,4-Dimethyl-9-phenoxytriptycene and its derivatives carrying a methyl, isopropyl, or *t*-butyl group in the *o*-position of the phenoxyl moiety were synthesized and their dynamic NMR behavior was studied. These molecules are considered to constitute a bevel gear system with a two-toothed and a three-toothed wheels and the dynamic NMR behavior is best explained in terms of gear rotation. The *o*-isopropyl derivative, for example, shows the energy barriers of 17.2 and 10.8 kcal† mol$^{-1}$ for the $ap \rightleftharpoons \pm sc$ and $+sc \rightleftharpoons -sc$ gearing processes, respectively. The population of the ±*sc* rotamer increases with the bulkiness of the *o*-alkyl group: The steric congestion among the *o*-alkyl group, the oxygen atom, and the *peri*-methyl group is severer in *ap* than in ±*sc*. Results of molecular mechanics calculations on these molecules are discussed.

In the course of our studies on restricted rotation about the bridgehead-to-substituent bond in 9-substituted triptycene derivatives,[2)] we have been interested in the stereodynamics of 9-benzyltriptycene (**1**) and its various derivatives.[3—7)]

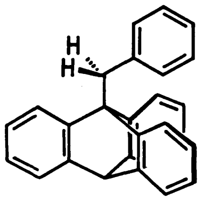

**1**

Compound **1** adopts a conformation in which the plane of the phenyl group is coplanar with the bridgehead-to-methylene bond and thus constitutes a meshed bevel gear with a two-toothed and a three-toothed wheels. Dynamic NMR studies of singly *peri*-substituted 9-(2-methylbenzyl)triptycenes (**2**)[6)] and 9-(2,4,6-trimethylbenzyl)triptycenes (**3**)[7)] revealed that these molecules behave as dynamic gears: Gear rotation is the lowest energy process and gear slippage has a higher barrier. Mislow *et al.*[8)] made detailed molecular mechanics studies on the stereodynamics of **1**, 9-(2,6-dimethylbenzyl)triptycene, and its 1-methyl derivative, which are complementary to our results.

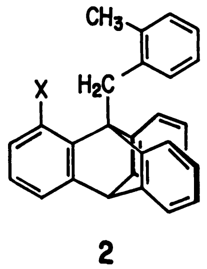

**2**

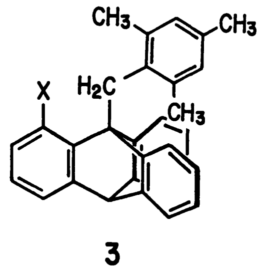

**3**

It was reasonably expected that observation of gear rotation could be extended to systems where the methylene group in 9-(arylmethyl)triptycenes is replaced by a heteroatom group such as O, NH, and so on, and that it would be of interest to see how the stereodynamics of these compounds differs from that of the carbon analogs. We report here NMR studies on the stereodynamics of 1,4-dimethyl-9-phenoxytriptycene (**4**) and its derivatives (**5**—**7**) carrying an alkyl group in the *o*-position of the phenoxyl moiety.[9)] We discuss also the results of molecular mechanics calculations on these molecules.

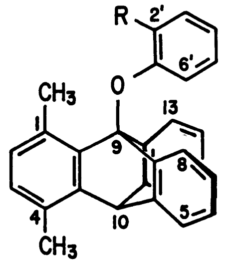

**4**: R=H
**5**: R=$CH_3$
**6**: R=$CH(CH_3)_2$
**7**: R=$C(CH_3)_3$

## Results and Discussion

*Syntheses.* The triptycenes **4**—**7** were synthesized by reactions of 9-aryloxyanthracenes (**8**—**11**) with 3,6-dimethylbenzyne. The anthracenes were obtained by Ullmann reactions from 9-bromoanthracene and appropriate phenols[10)] (Method A). Compounds **9** and **10** were prepared also by

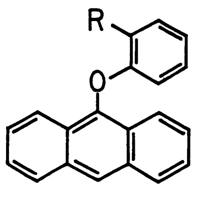

**8**: R=H
**9**: R=$CH_3$
**10**: R=$CH(CH_3)_2$
**11**: R=$C(CH_3)_3$

---

† 1 cal=4.184 J.

condensation of anthrone with the corresponding phenols in the presence of acid catalyst by the analogy of the recent report on the syntheses of 9-alkoxyanthracenes from anthrone and alcohols[11] (Method B). An attempt at the synthesis of **11** by the second method was not successful probably because of partial dealkylation under the reaction conditions.

*NMR Spectral Studies.* On the analogy of the behavior observed in 9-(2-methylbenzyl)triptycenes (**2**),[6] the stereodynamic behavior of **5**—**7** is expected to be explained in terms of the gear rotational circuit shown in Fig. 1.

Molecules of **5**—**7** exist as one of the three stable conformers, *ap*, +*sc*, and −*sc*, in which the *o*-alkyl group points toward outside of the triptycene skeleton. Conformers with the *o*-alkyl group pointing inwards, *ap*′, +*sc*′, and −*sc*′, are very unstable and populated too little to be detected, but serve as intermediates in the interconversion among the stable conformers by gear rotation (GR). The +*sc* rotamer changes to *ap*′ by a GR step in which the aryl group passes over a *peri*-hydrogen. We refer to this step as GR(H). As *ap*′ is unstable, the molecule immediately changes to −*sc* by further GR(H). Thus +*sc* and −*sc* interconvert by two successive GR(H) steps. In order for the +*sc* rotamer to convert to *ap*, it should first change to −*sc*′ by passing of the aryl group over the *peri*-methyl group, which we refer to as GR($CH_3$), and then to *ap* by GR(H). GR($CH_3$) should naturally have a higher energy barrier than GR(H) and therefore the $ap \rightleftharpoons \pm sc$ process should show a higher overall barrier than the $+sc \rightleftharpoons -sc$ process.

From the discussion above, the following behavior is expected in the dynamic NMR spectra. At low temperatures where both processes are frozen on the NMR time scale, the *ap* and ±*sc* rotamers are separately observed, and the chiral nature of the ±*sc* rotamer is proved by the diastereotopicity of a prochiral group such as $-CX_2Y$, if the molecule carries such a group. At an intermediate temperature range, the situation is realized where the $+sc \rightleftharpoons ap' \rightleftharpoons -sc$ occurs fast on the NMR time scale but the $+sc \rightleftharpoons -sc' \rightleftharpoons ap$ (and $-sc \rightleftharpoons +sc' \rightleftharpoons ap$) process is still slow.[12] In such circumstances, two rotamers are separately observed but the ±*sc* rotamer appears achiral in the NMR spectra. At higher temperatures where both processes occur fast on the NMR time scale, identity of the rotamers is lost and a coalesced signal is observed.

The 2′-isopropyl derivative (**6**) serves as a typical example. In the $^1$H NMR spectrum at ambient temperature, two sets of signals are observed in an intensity ratio of *ca.* 1:2 corresponding to the presence of two types of rotamers, *ap* and ±*sc* (Table 1). Among the four singlets due to the aromatic methyl groups appearing at δ 2.0—3.0, the highest-field one is reasonably assigned to the 1-methyl group of the ±*sc* rotamer because this methyl group is susceptible to the diamagnetic ring current of the benzene ring in the aryloxyl moiety. Then the other signals can be uniquely assigned as shown in Table 1 on the basis of the relative intensities and the coalescence behavior observed upon raising the temperature: The major isomer is assigned to ±*sc*. Validity of the rotamer assignment in **6** is further confirmed by the low temperature NMR behavior of **6** described below. The isopropyl-methyl signals consist of two doublets, one from *ap* and the other from ±*sc*, indicating that the *gem*-dimethyl groups

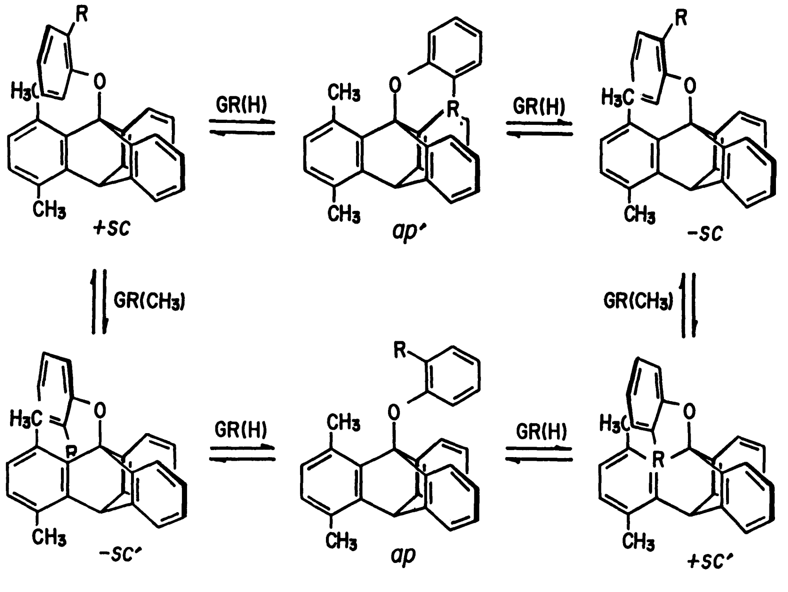

Fig. 1. Gear rotational circuit for 9-(2-alkylphenoxy)-1,4-dimethyltriptycenes.

are isochronous not only in *ap* but also in ±*sc*.

These spectral features are just those expected at intermediate temperatures mentioned above. Upon raising the temperature, the two sets of signals coalesce into an averaged set of signals, reflecting the increase of the interconversion rate between the *ap* and ±*sc* rotamers. Lineshape analysis of the 1- and 4-methyl proton signals obtained at 60 MHz in a chlorobenzene solution at five temperatures between 51 and 80 °C gave the rate constants for the process. The kinetic parameters obtained therefrom are shown in Table 2.

Meanwhile, upon lowering the temperature, the doublet signal assigned to the isopropyl-methyl group of the ±*sc* rotamer splits into two equally intense doublets, the other nonaromatic signals remaining intact. This feature suggests the slowdown of the $+sc \rightleftharpoons -sc$ process. The spectral change was studied at 400 MHz because no explicit splitting was observed at 60 MHz. At −81 °C in dichloromethane-$d_2$, the isopropyl-methyl signals appeared as three doublets at $\delta$=1.52, 1.48, and 1.46 with an intensity ratio of 29:29:42 indicating the presence of ±*sc* and *ap* in a ratio of 58:42.[13] Lineshape analysis of these signals in the temperature range of −60 to −25 °C afforded the rate con-

TABLE 1. 400 MHz $^1$H NMR DATA OF 9-ARYLOXY-1,4-DIMETHYLTRIPTYCENES (**4**—**7**) IN CDCl$_3$[a]

| Compd | Rotamer | Pop<br>% | 1-CH$_3$ | 4-CH$_3$ | 10-H | 5,16-H | 8,13-H | 2′-R | 6′-H |
|---|---|---|---|---|---|---|---|---|---|
| **4** | | | 2.779 | 2.443 | 5.630 | 7.426 d<br>(7.1) | 7.250 d<br>(7.1) | 7.38 br | 6.54 br |
| **5** | *ap* | 56 | 2.902 | 2.432 | 5.637 | 7.441 d<br>(7.1) | 7.140 d<br>(7.7) | 2.701 | 6.229 d<br>(8.1) |
| | ±*sc* | 44 | 2.035 | 2.552 | 5.621 | 7.363 ad<br>(≈7) | ≈7.44 br | 2.679 | 6.570 d<br>(8.1) |
| **6** | *ap* | 35 | 2.890 | 2.426 | 5.637 | 7.437 d<br>(8.1) | 7.134 d<br>(7.6) | 1.461 d<br>4.050 sep<br>(6.8) | 6.195 d<br>(8.3) |
| | ±*sc* | 65 | 2.090 | 2.550 | 5.618 | 7.406 dd<br>(7.6, 1.7) | ≈7.4 br | 1.511 d<br>3.921 sep<br>(6.8) | 6.600 dd<br>(7.8, 1.1) |
| **7** | ±*sc* | >98 | 2.139 | 2.556 | 5.617 | 7.291 d<br>(7.1)<br>7.439 d<br>(7.1) | 6.916 d<br>(7.6)<br>8.014 d<br>(7.6) | 1.754 | 6.651 dd<br>(8.3, 1.2) |

a) Obtained at 21—24 °C. Aromatic protons are omitted except for those shown in the Table. Chemical shifts are given in $\delta$. Signals are singlets unless otherwise stated; ad: apparent doublet, br: broad, d: doublet, dd: double doublet, sep: septet. In parentheses are coupling constants in Hz. The digital resolution of 0.24 Hz should be allowed for.

TABLE 2. DYNAMIC NMR DATA OF 9-ARYLOXYTRIPTYCENES (**4**—**7**) AND A RELATED COMPOUND (**15**)

| Compd | Process | Rds[a] | Signal Obsd | $T_c$<br>°C | $\Delta G^{\neq}(T)$<br>kcal mol$^{-1}$ (°C) | $\Delta H^{\neq}$<br>kcal mol$^{-1}$ | $\Delta S^{\neq}$<br>cal mol$^{-1}$ K$^{-1}$ | $K$[b] | MF[c]<br>MHz | Solvent |
|---|---|---|---|---|---|---|---|---|---|---|
| **4** | $ap \rightarrow \pm sc$ | GR(H) | 1,4-CH$_3$ | < −101 | <8.0 | | | | 400 | CD$_2$Cl$_2$ |
| **5** | $ap \rightarrow \pm sc$ | GR(CH$_3$) | 1-CH$_3$<br>4-CH$_3$ | ≈90<br>57 | 18.1 (60) | 18.7±0.3 | 1.8±1.4 | 0.92 | 60 | C$_6$H$_5$Cl |
| | $+sc \rightleftharpoons -sc$ | GR(H) | 8,13-H | ≈ −30 | 10.5 (−30) | | | | 400 | CDCl$_3$ |
| **6** | $ap \rightarrow \pm sc$ | GR(CH$_3$) | 1-CH$_3$<br>4-CH$_3$ | 87<br>59 | 18.2 (60) | 17.2±1.5 | −3.0±4.3 | 2.0 | 60 | C$_6$H$_5$Cl |
| | $+sc \rightleftharpoons -sc$ | GR(H) | CH(C*H*$_3$)$_2$ | ≈ −45 | 11.7 (−45) | 10.8±0.2 | −4.0±1.0 | | 400 | CD$_2$Cl$_2$ |
| | | | 8,13-H | ≈ −10 | 11.8 (−10) | | | | | |
| **7** | $+sc \rightleftharpoons -sc$ | GR(H) | 5,16-H | ≫60 | ≫16.0 | | | | 400 | CDCl$_3$ |
| | | | 8,13-H | >120 | >19.5 | | | | 60 | CCl$_2$CCl$_2$ |
| **15** | $ap \rightarrow \pm sc$ | GR(CH$_3$) | CH$_2$ | 98 | 20.0 (98) | | | 1.2 | 60 | C$_6$D$_5$CD$_3$ |
| | $+sc \rightleftharpoons -sc$ | GR(H) | CH$_2$ | 14 | 14.1 (14) | | | | 60 | C$_6$D$_5$CD$_3$ |

a) Rate-determining step. b) [±*sc*]/[*ap*] at around $T_c$. c) Magnetic field strength.

stants for the $+sc \rightleftharpoons -sc$ interconversion and the Eyring parameters therefrom (Table 2).

The 2′-methyl compound (**5**) shows a similar spectral feature as **6** does. Each of the 1- and 4-methyl groups gives rise to two singlets with an intensity ratio of 56:44 at ambient temperature. From the chemical shift criteria mentioned above, the major isomer is assigned to *ap* (Table 1). These signals coalesce on raising the temperature and lineshape analysis of the spectra at six temperatures between 39 and 73 °C affords the kinetic parameters for the $ap \rightleftharpoons \pm sc$ process in **5** as shown in Table 2.

As compound **5** has no NMR sensor groups which would definitely detect the $+sc \rightleftharpoons -sc$ process, no clear information is easily obtained for the process in **5**. The spectra of the aromatic protons give some information on this point, which is described later.

In the $^1$H NMR spectrum of the 2′-*t*-butyl derivative (**7**) at ambient temperature, a single peak is observed for each of the 1-methyl, 4-methyl, and 2′-*t*-butyl groups. The chemical shifts of the signals due to the 1- and 4-methyl groups are very similar to those of the corresponding signals in the $\pm sc$ rotamers of **5** and **6**.[14] This strongly suggests that **7** exists almost exclusively as the $\pm sc$ rotamer. The 400 MHz spectrum of the aromatic proton region is rather simple and is easily analyzed: The spectrum consists of three sets of ABCD four-spin systems and one AB-quartet, indicating that the two unsubstituted *o*-benzeno bridges are not equivalent. This clearly confirms that **7** exists solely as $\pm sc$ rotamer and further that the $+sc \rightleftharpoons -sc$ process is frozen at ambient temperature. The spectrum was completely analyzed by use of the double resonance technique and the signals were assigned as shown in Scheme 1 by assuming that the lowest-field signal should derive from 13-H and the highest-field one from 6′-H. No significant change in the lineshape was observed up to 60 °C and thus the energy barrier to the $+sc \rightleftharpoons -sc$ gearing, *i.e.* GR(H), in **7** is concluded to be considerably higher than 16 kcal mol$^{-1}$. The value is still conservative. In the 60 MHz spectra, the doublet at $\delta$ 8.01 assigned to 13-H appears clearly separated from the other aromatic signals, and shows no significant change of its appearance up to 120 °C, indicating that the energy barrier to GR(H) is higher than 19.5 kcal mol$^{-1}$.

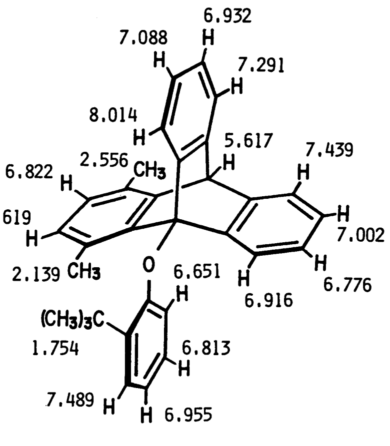

Scheme 1.

The aromatic proton spectra of **5** and **6** are far more complex than that of **7**, because **5** and **6** consist of two types of rotamers, *ap* and $\pm sc$. In these compounds, change in the lineshape in the aromatic region owing to the $+sc \rightleftharpoons -sc$ process was observed over a wide range of temperature, from −60 °C up to room temperature. Signals ascribed to 8-H and 13-H of the $\pm sc$ rotamer of **6** appearing at $\delta$ 7.90 and *ca.* 6.9 at −81 °C broadened on raising the temperature and coalesced at about −10 °C. The free energy of activation is roughly estimated to be 11.8±0.5 kcal mol$^{-1}$ using the approximate equation.[15] The value is consistent with the kinetic data obtained from the lineshape analysis of the isopropyl–methyl signals. The 2′-methyl compound (**5**) shows a similar signal broadening at somewhat lower temperatures than **6** does. The *peri*-protons coalesce at about −30 °C, which gives a rough $\Delta G^{\ddagger}$ value of 10.5±0.5 kcal mol$^{-1}$ for the $+sc \rightleftharpoons -sc$ process.

The transition state for the GR(H) step in the $+sc \rightleftharpoons -sc$ process would be represented by **12**. The severest steric interaction occurs between the face of the aryl group and the opposing *peri*-hydrogen. The energies of **12a** and **12b** will be similar because the *o*-substituent R can adopt a conformation in which an $\alpha$-hydrogen directs towards the triptycene skeleton, but the energy of **12c** will be considerably higher than those of **12a** and **12b**, because R has no $\alpha$-hydrogen in **12c**. Therefore it may be reasonable that the energy barriers to the $+sc \rightleftharpoons -sc$ process are similar for **5** and **6** but that for **7** is higher than those for **5** and **6**. Similarity of the GR(CH$_3$) barriers between **5** and **6** may be similarly understood.

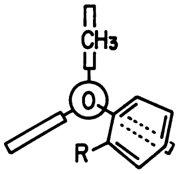

**12a** : $R = CH_3$
**12b** : $R = CH(CH_3)_2$
**12c** : $R = C(CH_3)_3$

It should be pointed out that the interconversion between *ap* and $\pm sc$ in **5** and **6** can occur by several other pathways. One group of such pathways involves an "isolated rotation" (IR) of the aryl group, which corresponds to slippage of the gear[4]: *ap* changes to *ap′* by IR and then to +*sc* (or −*sc*) by GR(H), or *ap* changes first to +*sc′* (or −*sc′*) by GR(H) and then to +*sc* (or −*sc*) by IR. In both pathways, IR is rate-determining. Inspection of molecular models, however, immediately suggests that the energy barrier to IR would be far higher than that to GR(CH$_3$) because the steric hindrance during the process is far larger. The transition state for IR seems something like **13** (the one for $ap \rightleftharpoons ap'$ is illustrated), in which the severest interactions occur between the *o*-groups (R or H) and the *peri*-hydrogens. The congestion around the *o*-substituent is far severer than that in the transition state for GR(H) or GR(CH$_3$), and thus the energy barrier to IR should be significantly dependent on the bulkiness of the *o*-substituent R. The similar barrier heights observed in **5** and **6** therefore strengthen the impression from the molecular model considerations that the pathways involving IR are not the lowest energy process for the $ap \rightleftharpoons \pm sc$ interconversion.[16]

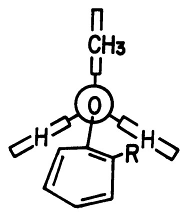

**13**

The possibility that any process involving the configurational inversion of the oxygen atom might be responsible for the dynamic NMR behavior is rejected by the facts that the $+sc \rightleftharpoons -sc$ and $ap \rightleftharpoons \pm sc$ processes are separately observed and that the energy barrier to the former process is far lower than that to the latter.[17]

Temperature dependence of the $^1$H NMR spectra of the 9-phenoxy compound (**4**) was studied as well at 400 MHz. In this molecule, the interconversion between *ap* and ±*sc* is attained by a single GR(H) step. At ambient temperature, one singlet is observed for each of the methyl groups, suggesting that the interconversion among rotamers is fast on the NMR time scale. The singlet at δ 2.44 is unambiguously assigned to the 4-methyl group by nuclear Overhauser effect (NOE) experiments: Upon irradiation of this signal, the bridgehead proton signal at δ 5.63 enhances its intensity by *ca.* 20%, while it remains intact on irradiation of the signal at δ 2.78. Even at −101 °C either of the methyl signals remains a singlet though somewhat broadened because of the slow-down of the process. Broadening of the 1-methyl signal is considerably larger than the 4-methyl signal and the peak height of the former is about a half of that of the latter at −101 °C. The larger broadening of the 1-methyl signal is reasonable because it should split into two peaks with a larger chemical shift difference than the 4-methyl signal on the analogy of the behavior found in **5** and **6**. Energy barrier to this process is estimated to be less than 8 kcal mol$^{-1}$.

Close inspection of the aromatic proton region of the spectra of **4** reveals an interesting phenomenon. Signals ascribed to two *o*-protons of the phenoxyl moiety appear as two multiplets at δ 6.32 snd 7.52 at −101 °C. The anisochrony of the *o*-protons remains even at room temperature, although the signals show considerable broadening. This means that any process which exchanges the magnetic environments of the two protons has a considerably high energy barrier of more than 15 kcal mol$^{-1}$. The to-and-fro gearing process ($+sc \rightleftharpoons ap' \rightleftharpoons -sc$) by two GR(H) does not average out the chemical shifts of the two protons. Either of two processes, GR(CH$_3$) and IR, can explain the observed dynamic NMR behavior. Differentiation between the two as the lower energy process is not possible at the present stage. Detailed studies along this line are in progress.

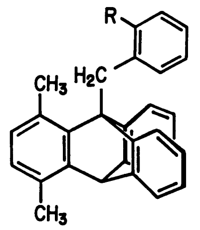

**14** : R = H
**15** : R = CH$_3$

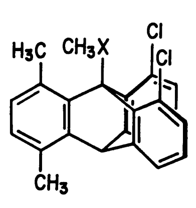

**16** : X = O
**17** : X = CH$_2$

In Table 2 are included the data for 1,4-dimethyl-9-(2-methylbenzyl)triptycene (**15**).[6] The rather small difference in the energy barriers between **5** and **15**, in both of those for GR(CH$_3$) and GR(H), is intriguing when one considers the large difference in the barriers to rotation about the triptycyl-X bond found in compounds **16** and **17**, where X is O and CH$_2$, respectively. The energy barriers to the $ap \rightleftharpoons \pm sc$ process, in which the methyl group in the 9-substituent eclipses one of the *peri*-chlorines in the transition state, were 11.8 and 20.2 kcal mol$^{-1}$ for **16** and **17**, respectively.[1,18]

As discussed in detail in the previous paper,[1] two main factors should be considered which govern the difference in rotational barriers between C–C and C–O bonds: (1) Three pairs of eclipsing interactions in the transition state for C–C rotation *vs.* one pair for C–O rotation, and (2) the difference in

TABLE 3. ROTAMER EQUILIBRIA OF **5** AND **6**

| Compd | Solvent | Temp Range °C | $\Delta H°$ kcal mol$^{-1}$ | $\Delta S°$ cal mol$^{-1}$ K$^{-1}$ | $K_{273}$a) |
|---|---|---|---|---|---|
| **5** | $CDCl_3$ | −24—58 | 0.73±0.17 | 2.1±0.6 | 0.77 |
| **6** | $CD_2Cl_2$ | −30—20 | 0.64±0.15 | 3.2±0.6 | 1.57 |

a) [±*sc*]/[*ap*].

TABLE 4. STERIC ENERGIES BY MM2 CALCULATIONS

| Compd | Rotamer | Rel. Energy kcal mol$^{-1}$ | Calcd Popul.a) % |
|---|---|---|---|
| **4** | *ap* | 0 | 97.8 |
| | ±*sc* | 2.67 | 2.2 |
| **5** | *ap* | 0 | 97.6 |
| | ±*sc* | 2.63 | 2.4 |
| | *ap′* | 9.08 | |
| | ±*sc′* | 10.81 | |
| **6** | *ap* **19a** | 0 | 95.1 |
| | **20a** | 0.18 | |
| | **21a** | 2.94 | |
| | ±*sc* **19b** | 2.35 | 4.9 |
| | **20b** | 2.21 | |
| | **21b** | 2.15 | |
| **7** | *ap* | 1.21 | 6.2 |
| | ±*sc* | 0 | 93.8 |

a) At 300 K. Statistical factors of conformers are properly taken into account.

bond length between C–C and C–O. The former factor operates to lower the C–O barrier. In the 9-$CH_3X$ system (**16** and **17**), the former factor contributes more strongly than the latter, resulting in the large barrier difference. In the aryl-X compounds (**5** and **15**), the latter factor would act to raise the C–O barrier, because the shorter C–X bonds increase the steric interaction between the face of the aryl group and the opposing *peri*-group (H or $CH_3$) in the transition state, while the effect would be less important in the ground state. Thus the second factor partly compensates the former factor to result in the small difference in the barriers.

*Rotamer Equilibria.* As shown in Table 1, the rotamer distribution is highly dependent on the *o*-alkyl group. Population of the *ap* rotamer steeply decreases as the *o*-alkyl group becomes bulkier. The van't Hoff parameters for **5** and **6** are given in Table 3.

Inspection of molecular models of 9-phenoxytriptycene indicates that the inner *o*-hydrogen in the phenoxyl moiety locates very closely to and thus strongly interacts with the triptycene skeleton. When a methyl group is present at a *peri*-position of the triptycene skeleton, it sterically interacts with the oxygen atom at the bridgehead. In the *ap* rotamer, the aryl group is pushed down into the notch made by the two *o*-benzeno bridges due to the buttressing effect of the *peri*-methyl group, which results in the destabilization of this isomer, but such an effect does not work in the ±*sc* rotamer. Presence of an alkyl group in the *o*-position increases the congestion and enhances the destabilization. Therefore, as the bulkiness of the *o*-alkyl group increases, the *ap* rotamer would be steeply destabilized, resulting in the increase in the population of the ±*sc* rotamer.

These situations seem to be reflected in $^1$H NMR spectra (Table 1). In the spectra of **5** and **6**, a doublet signal ascribed to 6′-H appears at the highest-field part of the aromatic proton region (*ca.* δ 6.2). No such signal is observed in the spectrum of **7**, in accordance with the absence of *ap* in **7**. The corresponding proton in the ±*sc* rotamer appears at a lower field of *ca.* δ 6.6 in **5**—**7**. The buttressing effect should push the proton into the shielding region of the flanking benzene rings in the *ap* rotamer.

Although the rotamers of **4** are not separately observed at room temperature or even at the lowest temperature examined (−101 °C), the populations can be roughly estimated from the averaged chemical shift of the 1-methyl signal. If it is assumed that the chemical shift of the 1-methyl protons for each rotamer is the same as that in **5**, *i.e.* δ 2.04 for ±*sc* and δ 2.90 for *ap*, the averaged value of δ 2.78 observed at 24 °C predicts the population of *ap*-**4** to be about 85% at this temperature. Predominance of the *ap* rotamer in **4** may be consistent with the extrapolation of the tendency observed in **5**—**7**, though the value seems somewhat larger than expected judging from the fact that, in the carbon analogs **14** and **15**, the population of *ap* decreases only slightly on going from **14** to **15** (54% in **14** at −50 °C in $CDCl_3$–$CS_2$ (2:3)3a) and 50% in **15** at −33 °C in $CDCl_3$6)).

*Molecular Mechanics Calculations.* In order to understand the dependence of rotamer equilibria upon the *o*-alkyl group in more detail, we performed molecular mechanics calculations on **4**—**7** using the MM2 force field.19) Relative steric energies of conformers are compiled in Table 4.

In any of the stable rotamers of **4**—**7**, the plane of the aryl moiety is coplanar with the $C_9$–O bond: The dihedral angles C(9)–O–C(1′)–C(6′) are less than ±3°, except for +*sc*-**7** where it is −6.6°. Two *o*-benzeno bridges flanking the aryl group bend away from each other, the dihedral angle C(1′)-O-C(9)-C being *ca.* 65°. The C(9)-O-C(1′) angles are around 121°, widening by about 10° from the standard C($sp^3$)-O-C($sp^2$) angle of 110.8°.

As for the conformation of the *o*-alkyl group, the conformation **18** in which a hydrogen or a methyl

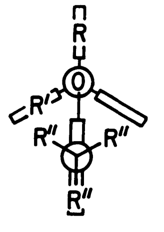

R or R′ = $CH_3$
R″ = H or $CH_3$

**18**

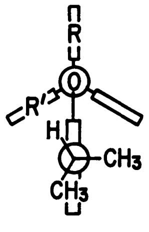

**19**

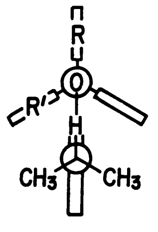

**20**

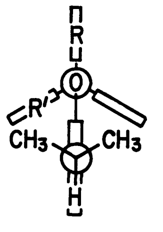

**21**

**a** : R = $CH_3$, R′ = H
**b** : R = H, R′ = $CH_3$

group eclipses 3′-C was calculated to be the most stable in either rotamer of **5** and **7**. In *ap*-**6**, the lowest-energy conformation is **19a** in which one of the methyl group is perpendicular to the plane of the benzene ring. Conformation **20a** is slightly less stable than **19a**. **21a** in which the methine hydrogen eclipses 3′-C is far less stable, because the *gem*-dimethyl groups are very close to the *peri*-methyl group. In +*sc*-**6**, on the other hand, **19b**, **20b**, and **21b** have almost the same energy.[20)]

Steric energies of the unstable rotamers with the *o*-alkyl group pointing inwards, *ap*′ and ±*sc*′, were calculated for **5**. *ap*′-**5** was shown to be less stable by 9.08 kcal $mol^{-1}$ than *ap*-**5**, and ±*sc*′-**5** less stable by 8.18 kcal $mol^{-1}$ than ±*sc*-**5**.

As is evident from Table 4, the steric energy of the ±*sc* rotamer relative to the corresponding *ap* one decreases on going from **5** to **6**, and in the *t*-butyl derivative **7**, ±*sc* is more stable than *ap*. The tendency that the ±*sc* rotamer becomes more and more populous as the *o*-substituent becomes bulkier is reproduced by calculation, but the quantitative agreement between the experiment and the calculation is very poor.

These discrepancies might be partly ascribed to solvent effects and/or some other factors which affect the relative energies of rotamers but are not reproduced by molecular mechanics calculations. One of such possibilities is the C-H···π attractive interaction, which might operate between the *peri*-methyl and the aryl groups in the ±*sc* rotamer.[21)] However, most of the discrepancies should be attributed to the intrinsic properties of the force field used. Overestimation of the steric energies of the ±*sc* rotamers, especially by overestimating the repulsive interaction between the *peri*-methyl group and the flanking aryl group in ±*sc*, seems to be the most probable origin. Similar situations were encountered by Mislow *et al.* in their molecular mechanics studies on the stereodynamics of 9-(arylmethyl)triptycenes.[8)] They found that the repulsive interaction between a benzene ring and a hydrogen which protrudes into the π-cloud of the benzene ring is overestimated in the calculations of the transition states for GR in 9-(arylmethyl)triptycenes and also for the ring flipping in [2.2]metaparacyclophane. Such overestimation seems to operate in the calculations of conformational equilibria as well.[8)]

It has become evident that the MM2 force field does not satisfactorily reproduce the conformational equilibria in our present compounds. Improvement of the force field and/or the calculation methodology is necessary to obtain satisfactory results on the ground states and to further extend the calculations to the energy surfaces of the dynamic processes, and is under investigation.[22)]

## Experimental

*Materials.* Yields, melting points, and the analytical data are compiled in Table 5. Melting points are not corrected.

*General Procedure for the Synthesis of 9-Aryloxyanthracenes. Method A.* A mixture of 2.57 g (10 mmol) of 9-bromoanthracene and 30 mmol of an appropriate phenol was heated at 220—230 °C for 4 h together with 1.0 g of potassium hydroxide and 0.3 g of copper powder. The reaction mixture was extracted with dichloromethane and the extract was washed with aqueous sodium hydroxide to remove the unreacted phenol and then with water, dried over magnesium sulfate and concentrated. The residue was chromatographed on silica gel with benzene-hexane as the eluent. Recrystallization of the eluate from tetrahydrofuran-hexane gave pure compounds. $^1$H NMR data of the anthracenes are given in Table 6.

*Method B.* A mixture of 3.88 g (20 mmol) of anthrone and 100 mmol of a phenol in 100 mL of toluene containing 1.0 mL of concentrated sulfuric acid was heated under reflux for 150—180 h using a Dean-Stark water collector. The reaction mixture was washed with aqueous sodium hydroxide and then with water, dried over magnesium sulfate, and concentrated. Chromatography on silica gel followed by recrystallization gave the anthracenes as above.

TABLE 5. YIELDS, MELTING POINTS, AND ANALYTICAL DATA

| Compd | Method | Yield | Mp | Found (%) | | Calcd (%) | |
|---|---|---|---|---|---|---|---|
| | | % | $\theta_m$/°C | C | H | C | H |
| **8** | A | 14 | 131—132[a] | | | | |
| **9** | A | 30 | 140—141 | 88.47 | 5.58 | 88.70 | 5.67 |
| | B | 36 | | | | | |
| **10** | A | 17 | 161—162 | 88.63 | 6.15 | 88.42 | 6.45 |
| | B | 38 | | | | | |
| **11** | A | 7 | 202—203 | 88.37 | 6.59 | 88.31 | 6.79 |
| **4** | | 28 | 202—203 | 90.04 | 5.64 | 89.80 | 5.92 |
| **5** | | 29 | 193—194 | 89.51 | 6.02 | 89.65 | 6.23 |
| **6** | | 31 | 162—163 | 89.33 | 6.64 | 89.38 | 6.78 |
| **7** | | 33 | 224—225 | 89.00 | 6.74 | 89.26 | 7.02 |

a) Lit: 132—133 °C (Ref. 10).

TABLE 6. $^1$H NMR DATA OF ANTHRACENES IN $CDCl_3$ AT *ca.* 35 °C[a]

| Compd | R | 2′-R | 6′-H | 10-H | Other Aromatic Protons |
|---|---|---|---|---|---|
| **8** | H | b) | b) | 8.35 s | 6.6—7.6(9H), 7.8—8.2(4H) |
| **9** | $CH_3$ | 2.71 s | 6.00m | 8.34 s | 6.6—7.0(2H), 7.1—7.6(5H), 7.8—8.2(4H) |
| **10** | $CH(CH_3)_2$ | 1.55 d<br>3.90 sep<br>($J$=6.9 Hz) | 5.99m | 8.35 s | 6.6—7.0(2H), 7.1—7.6(5H), 7.8—8.2(4H) |
| **11** | $C(CH_3)_3$ | 1.76 s | 6.00m | 8.36 s | 6.6—7.0(2H), 7.2—7.6(5H), 7.8—8.2(4H) |

a) Obtained at 90 MHz. Chemical shifts are given in δ. b) Not identified.

*General Procedure for the Synthesis of 9-Aryloxy-1,4-dimethyltriptycenes.* A solution of 830 mg (5 mmol) of 3,6-dimethylanthranilic acid[23] in 20 mL of 1,2-dimethoxyethane (DME) and a solution of 1.0 mL (*ca.* 7.5 mmol) of isopentyl nitrite in 10 mL of DME were added dropwise during the course of 1 h to a boiling solution of 2.0 mmol of 9-aryloxyanthracene in 20 mL of DME so that an excess of isopentyl nitrite was always present in the reaction mixture. The reaction mixture was heated under reflux for further 30 min and concentrated. Chromatography of the residue on silica gel with hexane as the eluent followed by recrystallization from tetrahydrofuran–hexane gave the desired triptycene as colorless crystals.

*Spectral Measurements.* $^1$H NMR spectra at ambient temperature and below were obtained on a JEOL GX-400 spectrometer operating at 399.65 MHz in the pulse FT mode. Temperatures were read as digital outputs from the variable temperature accessory and are not corrected. Dynamic NMR spectra above room temperature were obtained on a Hitachi R-20B spectrometer at 60.0 MHz in the CW mode, and temperatures were calibrated using ethylene glycol.[24] Measurements of some of the spectra at ambient temperature as well as the nuclear Overhauser effect experiments were made on a Varian EM-390 spectrometer at 90.0 MHz in the CW mode.

*Computer Simulations.* Theoretical spectra were obtained on a HITAC M-280H computer system at the Computer Center of The University of Tokyo (CCUT) using a modified version of the DNMR3 program by Binsch.[25] Temperature dependence of the isopropyl-methyl signals of **6** was analyzed as a 3-spin 3-site system ($ABX \rightleftarrows BAX \rightleftarrows C_2Y$) instead of a 7-spin 3-site system ($A_3B_3X \rightleftarrows B_3A_3X \rightleftarrows C_6Y$), regarding a methyl group as a single nucleus. In this case, the rate constant for the ±*sc*→*ap* process, *i.e.* $ABX \rightarrow C_2Y$ and $BAX \rightarrow C_2Y$, was assumed to be 0.001 $s^{-1}$ throughout the temperature range of −60 to −25 °C (see Ref 13). The spectra of the 1- and 4-methyl groups in **5** and **6** were simulated as a 2-spin 2-site system ($AB \rightleftarrows CD$), regarding again a methyl group as a single nucleus.

*Molecular Mechanics Calculations.* Calculations were performed on the HITAC M-280H computer system using the MM2 program in the CCUT Program Library. Original parameters in the program were used as they were except for the bond length and the stretching force constant for $C(sp^2)$–$C(sp^2)$, which were modified so that they represented aromatic carbons ($l_0$=1.3937 Å, $k_s$=8.067 mdyn[††] $Å^{-1}$). Only one set of torsional parameters were newly added: $V_1=V_2=V_4=0$, $V_3$=0.403 kcal $mol^{-1}$ for $C(sp^2)$–$C(sp^3)$–O–$C(sp^2)$.

The authors are grateful to Professors N. L. Allinger and E. Ōsawa for their helpful discussion, and to Dr. G. Izumi of Nippon Kayaku Co., Ltd. and Mr. S. Murata of Institute for Molecular Science for the measurements of the 400 MHz $^1$H NMR spectra.

---

[††] 1 dyn=$10^{-5}$ N.

## References.

1) Part LVI: G. Yamamoto and M. Ōki, *Bull. Chem. Soc. Jpn.*, **58**, 1690 (1985).

2) M. Ōki, *Angew. Chem., Int. Ed. Engl.*, **15**, 87 (1976).

3) a) F. Suzuki and M. Ōki, *Tetrahedron Lett.*, **1974**, 2845; *Bull. Chem. Soc. Jpn.*, **48**, 596 (1975); b) M. Kono, H. Kihara, N. Nakamura, F. Suzuki, and M. Ōki, *ibid.*, **52**, 1682 (1979); M. Ōki, M. Kono, H. Kihara, N. Nakamura, *ibid.*, **52**, 1686 (1979).

4) G. Yamamoto, *J. Mol. Struct.*, **126**, 413 (1985).

5) G. Yamamoto and M. Ōki, *Chem. Lett.*, **1979**, 1251; *Bull. Chem. Soc. Jpn.*, **54**, 473 (1981).

6) G. Yamamoto and M. Ōki, *Chem. Lett.*, **1979**, 1255; *Bull. Chem. Soc. Jpn.*, **54**, 481 (1981).

7) G. Yamamoto and M. Ōki, *J. Org. Chem.*, **48**, 1233 (1983).

8) R. B. Nachbar, Jr., W. D. Hounshell, V. A. Naman, O. Wennerström, A. Guenzi, and K. Mislow, *J. Org. Chem.*, **48**, 1227 (1983).

9) Preliminary results have been reported: G. Yamamoto and M. Ōki, *Chem. Lett.*, **1984**, 97.

10) W. Theilacker, U. Berger-Brose, and K.-H. Beyer, *Chem. Ber.*, **93**, 1658 (1960).

11) W. H. Pirkle and J. M. Finn, *J. Org. Chem.*, **48**, 2779 (1983).

12) In this temperature range, the *ap* rotamer may be in dynamic equilibrium with ±*sc′* although the situation is not detected by NMR because the population of ±*sc′* is extremely low. Similarly, the GR(H) barrier in *ap* $\rightleftharpoons$ ±*sc′* is not obtained experimentally.

13) The ratio does not necessarily represent the equilibrium populations at −81 °C: The data in Table 3 indicate that the value corresponds to the equilibrium populations at about −30 °C. The *ap* $\rightleftharpoons$ ±*sc* process is very slow in this temperature range and the equilibrium might not have been attained during the NMR measurements. The nonequilibrium state, however, does not affect the analysis of the +*sc* $\rightleftharpoons$ −*sc* process.

14) Nuclear Overhauser effect experiments confirmed that the low-field signal at $\delta$ 2.56 derives from 4-CH$_3$: irradiation of this signal enhances the intensity of the 10-H signal at $\delta$ 5.62 by *ca.* 20% while irradiation at $\delta$ 2.14 does not change the 10-H signal intensity.

15) D. Kost, E. H. Carlson, and M. Raban, *J. Chem. Soc., Chem. Commun.*, **1971**, 656.

16) Molecular mechanics studies would afford some information on these points but are still pending for several reasons discussed in the later section.

17) For further discussion on this point, see Ref. 1.

18) G. Yamamoto and M. Ōki, *Bull. Chem. Soc. Jpn.*, **57**, 2219 (1984).

19) N. L. Allinger, *J. Am. Chem. Soc.*, **99**, 8127 (1977); N. L. Allinger and Y. H. Yuh, *QCPE*, No. 395.

20) For conformational analysis of an isopropyl group in substituted cumenes and related compounds, see for example: A. Mannschreck and L. Ernst, *Chem. Ber.*, **104**, 228 (1971); C. Roussel, A. T. Balaban, U. Berg, M. Chanon, R. Gallo, G. Klatte, J. A. Memiaghe, J. Metzger, D. Oniciu, and J. Pierrot-Sanders, *Tetrahedron*, **39**, 4209 (1983); J. C. Schug and J. W. Viers, *ibid.*, **40**, 3971 (1984).

21) See for example: S. Zushi, Y. Kodama, K. Nishihata, K. Umemura, M.Nishio, J. Uzawa, and M. Hirota, *Bull. Chem. Soc. Jpn.*, **53**, 3631 (1980).

22) For example, the use of smaller values for the van der Waals radius ($r^*$) of an sp$^2$-carbon was found to improve the situation. When the radius of 1.50 Å was used instead of the original value of 1.94 Å, the energy difference between *ap*-**5** and ±*sc*-**5** was 1.45 kcal mol$^{-1}$ favoring *ap*-**5**. It is however uncertain whether the single change of $r^*$(sp$^2$-C) gives the totally consistent results not only for the energy differences of rotamers but also for the molecular geometries.

23) S. Gronowitz and G. Hansen, *Arkiv Kemi*, **27**, 145 (1967); M. S. Newman and J. A. Cella, *J. Org. Chem.*, **38**, 3482 (1973).

24) A. L. Van Geet, *Anal. Chem.*, **40**, 2227 (1968).

25) G. Binsch, *Top. Stereochem.*, **3**, 97 (1968); D. A. Kleier and G. Binsch, *QCPE*, No. 165.